

(2)

ADSORPTION, MOBILITY AND ORGANISATION OF
ORGANIC MOLECULES AT CLAY SURFACES PROBED BY
PHOTOPHYSICS AND PHOTOCHEMISTRY

AD-A218 490

Final report

December, 15 1989

DTIC
ELECTED
FEB 13 1990
S B D
P

United States Army
European Research Office of the U.S. Army
London, England

Unclassified

SECURITY CLASSIFICATION OF THIS PAGE

REPORT DOCUMENTATION PAGE				Form Approved OMB No 0704-0188 Exp Date: Jun 30, 1986
1a. REPORT SECURITY CLASSIFICATION Unclassified		1b. RESTRICTIVE MARKINGS		
2a. SECURITY CLASSIFICATION AUTHORITY		3. DISTRIBUTION/AVAILABILITY OF REPORT Approved for public release; distribution unlimited		
2b. DECLASSIFICATION/DOWNGRADING SCHEDULE				
4. PERFORMING ORGANIZATION REPORT NUMBER(S)		5. MONITORING ORGANIZATION REPORT NUMBER(S)		
6a. NAME OF PERFORMING ORGANIZATION Catholic University		6b. OFFICE SYMBOL (If applicable)	7a. NAME OF MONITORING ORGANIZATION USARDSG-UK, U.S. Army European Research Office	
6c. ADDRESS (City, State, and ZIP Code) Department Scheikunde, Celestijnenlaan 200F, B-3030 Heverlee-Leuven, Belgium		7b. ADDRESS (City, State, and ZIP Code) P.O. Box 65 FPO NY 09510-1500		
8a. NAME OF FUNDING/SPONSORING ORGANIZATION U.S. Army European Research Office		8b. OFFICE SYMBOL (If applicable)	9. PROCUREMENT INSTRUMENT IDENTIFICATION NUMBER DAJA45-87-C-0006	
8c. ADDRESS (City, State, and ZIP Code) USARDSG-UK Box 65 FPO NY 09510-1500		10. SOURCE OF FUNDING NUMBERS		
		PROGRAM ELEMENT NO. 61103A	PROJECT NO. 1L161103BH57	TASK NO. 08
		WORK UNIT ACCESSION NO.		
11. TITLE (Include Security Classification) (U) Organization of Organic Molecules at Clay Surfaces.				
12. PERSONAL AUTHOR(S) Dr. F.C. de Schryver				
13a. TYPE OF REPORT Final	13b. TIME COVERED FROM 86-12-10 TO 89-12-10	14. DATE OF REPORT (Year, Month, Day) 89-12-15	15. PAGE COUNT 36	
16. SUPPLEMENTARY NOTATION The view, opinions and/or findings contained in this report are those of the author(s) and should not be construed as an official Department of the Army position, policy or decision unless so designated by other documentation.				
17. COSATI CODES		18. SUBJECT TERMS (Continue on reverse if necessary and identify by block number) Adsorption, clay, mobility, surfactant, pyrene, fractal analysis, photophysics, photochemistry, ORGANIC COMPOUNDS, LAPONITE CLAY, FLUORESCENCE, ANISOTROPY.		
FIELD 07	GROUP 04			
19. ABSTRACT (Continue on reverse if necessary and identify by block number) A new approach to the problem of the fluorescence decay of molecules adsorbed on surfaces is offered by the use of the expression developed by Klafter and Blumen which describes the Förster energy transfer in a fractal environment. A simulation study was conducted to find out how to best analyze an anisotropic decay. It was found that the inclusion of more than two analyzer angles did not improve the analysis dramatically. Some of the photophysical properties of 3-(1-pyrenyl)propyl trimethylammonium bromide (P3N) adsorbed on commercially available silica colloid, Ludox, were investigated. Adsorption and mobility of P3N in the presence of co-adsorbed CTAC were studied using photostationary fluorescence and single-photon-timing. Silica was derivatized with polyethylene glycol dimethylacrylate and the polymerization of the acrylate was investigated. Absorbance measurements of P3N adsorbed on Laponite clay as a function of Laponite concentration was studied. The ratio of intensities of the second and the third band of the pyrenyl group of P3N increases as the Laponite concentration increases. This effect is said to be due to a different degree of intermolecular interaction between the chromophores at the different Laponite concentrations.				
20. DISTRIBUTION/AVAILABILITY OF ABSTRACT <input checked="" type="checkbox"/> UNCLASSIFIED/UNLIMITED <input type="checkbox"/> SAME AS RPT. <input type="checkbox"/> DTIC USERS		21. ABSTRACT SECURITY CLASSIFICATION Unclassified		
22a. NAME OF RESPONSIBLE INDIVIDUAL Dr. R.P. Seiders		22b. TELEPHONE (Include Area Code) 071-409 4423	22c. OFFICE SYMBOL AMXSN-UK-RC	

TABLE OF CONTENTS

1. STUDY OF THE FLUORESCENCE DECAY OF MOLECULES ADSORBED ON SURFACES.
2. ADSORPTION OF ORGANIC MOLECULES ON SILICA COLLOIDS
3. SYNTHESIS OF SILICA DERIVATISED WITH A WATER SOLUBLE POLYMER WITH AN UNSATURATED METHACRYLIC BOUND AS END GROUP
4. ADSORPTION AND POLYMERIZATION OF DETERGENTS AT A CLAY SURFACE
5. REFERENCES



Accession For	
NTIS GRA&I	<input checked="" type="checkbox"/>
DTIC TAB	<input type="checkbox"/>
Unannounced	<input type="checkbox"/>
Justification	
By _____	
Distribution/ _____	
Availability Codes	
Dist	Avail and/or Special
A-1	

1. STUDY OF THE FLUORESCENCE DECAY OF MOLECULES ADSORBED ON SURFACES.

1.1. Introduction.

In general the interpretation of the fluorescence decays of molecules adsorbed on various surfaces (silica, alumina, zeolites, monolayers, clays) is not unambiguous. The time-dependent fluorescence of the organo-clay systems, has also been studied. Several functions have been used to describe the fluorescence decays of adsorbed probe molecules on a clay surface. : one-exponential ⁽¹⁾, two-exponential ⁽²⁾, Poisson distribution of lifetimes ⁽³⁾, three-exponential ⁽⁴⁾.

Adsorbed molecules aggregate on the clay surface. This means that besides monomers, several aggregates (dimer, trimer, ...) are present on the surface. Energy transfer from a single monomeric molecule to the aggregates can thus occur. In addition, these aggregates can form excimers upon excitation. Therefore a very complicated fluorescence decay can be expected.

The distribution of the adsorbed molecules can be changed by co-adsorbing detergentmolecules with a sufficient chain length,.

As reported previously the aggregation of the probe molecules decreases with increasing detergent concentration.

The fluorescence decay of the pyrene probe becomes less complex when detergent molecules are co-adsorbed. One possible approach is to use a two-exponential function to fit the fluorescence decay. Besides the monomer lifetime, a short decay time is observed. The contribution of the short decay time decreases with increasing detergent concentration. The fluorescence decay becomes thus more and more one-exponential with increasing detergent concentration but, even at the highest detergentconcentration a multi-exponential function is needed to describe the fluorescence decay.

In a certain region of concentration one can succesfully apply micellar kinetics to describe the fluorescence decay, as is shown in a previous report.

When there is no detergent co-adsorbed the fluorescence decay of the adsorbed probe is very complicated. Here a three-exponential function is sometimes used to fit the decay. Short decay components are found besides the monomer fluorescence lifetime. These short decay components are usually ascribed to the aggregates.

However there exist no underlying model to explain this three-exponential behaviour.

1.2. Simulations of fluorescence decays using the fractal concept

1.2.1. Introduction

A new approach to the problem of the fluorescence decay of molecules adsorbed on surfaces is offered by the use of the expression developed by Klafter and Blumen which describes the Förster energy transfer in a fractal environment.

The notion "fractal" was first used by Mandelbrot to describe geometrical structures whose dimensions have non-integer values.⁽⁵⁾ Fractals have the potential to describe a multitude of irregular structures. All of these structures are then characterized by a fractal dimension D. With the aid of this fractal dimension it is possible to distinguish between different irregular structures in a more or less quantitative manner.

As mentioned before an expression was derived by Klafter and Blumen for the Förster energy transfer from a donor molecule to a set of acceptor molecules which are randomly distributed on a fractal surface.⁽⁶⁾

$$\Phi(t) = \exp[-t/\tau_D - \gamma_A (t/\tau_D)^\beta]$$

$$\text{where } \beta = D/s \quad \text{and} \quad \gamma_A = x_A (d/D) V_d R_0^D \Gamma(1-\beta)$$

τ_D is the lifetime of the donor molecule and s is the order of the multipolar interaction (6 in the case of dipolar interactions); x_A is the fraction of fractal sites occupied by an acceptor; d and D are the Euclidean and fractal dimension respectively; R_0 is the critical transfer distance; V_d is the volume of a unit sphere in d-dimensions; and $\Gamma(1-\beta)$ is the gamma Euler function of (1-β).

This expression is now used intensively in different heterogeneous systems e.a. in vesicles and on irregular surfaces.^(7,8)

Before using it on our own systems we want to investigate by a computer simulation study to what extent it is possible to analyse this expression unambiguously.

A fractal decay is hereby simulated and then analysed by different expressions e.a. multi-exponential decay and expressions derived for fluorescence quenching in micellar systems. All of these expressions have been proposed in the past to describe the fluorescence decay of adsorbed molecules.

Also the decays obeying these other expressions will be simulated and then analysed by the expression proposed by Klafter and Blumen.

By using this procedure one can determine if it is possible to distinguish between the different models and find the conditions where this is at best possible.

1.2.2. Method

The simulated decays are obtained by convoluting the decay as predicted by the expressions with a non smoothed measured instrument response function and adding Poisson noise to this. The time increment and the pre-exponential factors are chosen carefully so that the number of counts in the peak channel is about 10,000 and the generated curve decays over at least 2 decades.

The decays are analyzed by a non linear least square method based on the Marquardt algoritme.⁽⁹⁾ The goodness of fit is evaluated by a number of statistical tests. (χ^2 z χ^2 ordinary runs, Durbin Watson).

As a tool for the analysis we use the global analysis program developed in the laboratory. In a global analysis experiment one analyses different decays at the same time taking into account the existing relationships between parameters, based on a model and thus reducing the total amount of parameters. In this way a better precision and an improved modeltesting capability is achieved.

1.2.3. Results

Different sets of experiments were simulated utilizing the expression derived by Klafer and Blumen. Afterwards these experiments are analyzed in different ways : as a mono-exponential, a two exponential or a three exponential decay. Both with single curve analysis and with global analysis it turns out to be impossible to fit a fractal decay to a mono exponential or a two exponential decay.

A three exponential fit to the fractal data gave good fits with single

curve analysis and this over the whole of the concentration region studied. A global analysis, which makes use of model dependent relations between the parameters, can help to distinguish between the models.

Micellar kinetics, which is another often used approach for the analysis of the fluorescence decays of adsorbed dyes can easily be distinguished from a fractal decay both with single curve analysis and with the global analysis approach.

Finally, an expression used in the analysis of energy transfer between dyes in monolayers was tested against the fractal analysis.

$$\Phi(t) = A_1 \exp[-t/\tau_D - q_A(t/\tau_D)^{1/3}] + A_2 \exp(-t/\tau_D)$$

The expression consists out of two parts : one is the generally known expression for Förster energy transfer in two dimensions the other part is a mono-exponential decay. This expression is used to analyze energy transfer in monolayers and is explained by the concept of domain formation in the monolayers.⁽¹⁰⁾ The mono-exponential part is then ascribed to the decay of isolated donors far from the acceptors which reside in an other domain of the monolayer. The simulation study clearly showed that this expression could not be fitted to a fractal decay and this for a set of experiments were the ratio of the pre-exponential factors ranged from 0.1 % till 1 %.

1.3. Analysis of the time dependent emission anisotropy

1.3.1. Introduction.

1.3.1.1. DEFINITIONS

If the excitation beam is vertically polarized, the polarisation (11) $p(t)$ is given by :

$$p(t) = \frac{i_{\parallel}(t) - i_{\perp}(t)}{i_{\parallel}(t) + i_{\perp}(t)}$$

with $i_{\parallel}(t)$ the intensity in the horizontal plane and $i_{\perp}(t)$ the intensity in the vertical plane.

The anisotropy (12) $r(t)$ is then given by :

$$r(t) = \frac{i_{\parallel}(t) - i_{\perp}(t)}{i_{\parallel}(t) + 2 i_{\perp}(t)}$$

The anisotropy $r(t)$ has the advantage that it is independent of the fluorescence of the chromophor as it contains the expression for the total fluorescence $f(t)$.

$$f(t) = i_{\parallel}(t) + 2 i_{\perp}(t)$$

The foregoing expressions can be written as :

$$i_{\parallel}(t) = 1/3 f(t) [1 + 2 r(t)]$$

$$i_{\perp}(t) = 1/3 f(t) [1 - r(t)]$$

Or, in general, for every angle θ of the analyser, if one excites with vertical polarized light, :

$$i(\theta, t) = 1/3 f(t) [1 + (3\cos^2\theta - 1)r(t)]$$

If the analyser is set at $\theta = 54.7^\circ$, the so called magic angle, $(3\cos^2\theta - 1) = 0$ and the observed decay is proportional with the total fluorescence decay. Almost all of the earlier presented data was taken under this condition to exclude any anisotropy effect.

1.3.1.2. UNDERLYING PRINCIPLES.

The probability of absorption P_{abs} is given by :

$$P_{abs} \sim |\mu_a \cdot E|^2$$

with E the electric field vector of the excitation beam and μ_a the absorption dipole.

If the excitation light is plane polarised a photoselection of the chromophors is the result. An analogue expression can be written for the probability of emission P_{em} :

$$P_{em} \sim |\mu_e \cdot E'|^2$$

with E' the electric field vector of the emitted wave and μ_e the emission dipole.

In the fluorophor the emission dipole moment has a fixed orientation with respect to the absorption dipole .The macroscopic fluorescence of the selected ensemble of fluorophors will be polarized.

Every process that leads to a more uniform distribution of the emission dipoles will then result in a decrease of the polarisation. The two most important processes are the rotational movement of the chromophor and the energy transfer between the chromophors.

The analysis of the time dependent anisotropy can thus give information about the rotational freedom of the adsorbed molecules and

is an alternative way to measure the energy transfer processes that take place between the adsorbed chromophors. With this method it's perfectly possible to measure donor donor energy migration.

1.3.2. Experimental determination of the anisotropy.

The time dependent anisotropie is traditionally determined out of the experimentally observable decays $I_{\parallel}(t)$ and $I_{\perp}(t)$.

The sum $S(t)$ and difference $D(t)$ curves are calculated :

$$S(t) = I_{\parallel}(t) + 2\alpha I_{\perp}(t)$$

$$D(t) = I_{\parallel}(t) - \alpha I_{\perp}(t)$$

α is a scaling factor which takes into account the fluctuations in the excitation pulse intensity and the different experimental conditions e.g. counting time ,the polarisation dependence of the photomultiplier etc.

The sum curve gives the total fluorescence decay $f(t)$ and the difference curve gives the product of the fluorescence decay $f(t)$ with the time dependent anisotropy $r(t)$: $D(t) = f(t)r(t)$. The analysis of the sum curve gives then the parameter values of the total fluorescence decay. These parameter values are then kept constant during the analysis of the difference curve which gives the parameter values of the emission anisotropy.

Sometimes one constructs the anisotropy "point by point" out of both curves.

$$R(t) = \frac{D(t)}{S(t)}$$

Disadvantages of this procedure are the necessity to determine the scaling factor α , the correct weighting factors for the different data

points have to be determined and the difficulties that arise in the deconvolution of the instrument response function. For a succesfull deconvolution of the sum and difference curves the instrument response functions of both $I_{\parallel}(t)$ and $I_{\perp}(t)$ have to be the same.

A new alternative approach to the problem is the simultaneous analysis of $I_{\parallel}(t)$ and $I_{\perp}(t)$ (13,14). As is mentioned before :

$$i_{\parallel}(t) = 1/3 f(t) [1 + 2 r(t)]$$

$$i_{\perp}(t) = 1/3 f(t) [1 - r(t)]$$

All parameters, both those of the total fluorescence decay and those of the time dependent emission anisotropy can be "linked" over the two curves with a global analysis program.

This method has a number of advantages : the convolution can be carried out as before without any need to have matched excitation profiles, Poisson statistics can be used, so the weighting factors are known. All of the parameters are calculated at the same time : the optimisation of the $r(t)$ parameters does not depend on previously calculated $f(t)$ parameters.

Because the linking involves system dependent parameters and not the actual data is it possible to measure both curves under different experimental conditions without the need to determine a scaling factor in a separate experiment. In the global analysis an additional parameter takes care of this scaling.

This global analysis approach can be further extended. Different sets of $I_{\parallel}(t)$ and $I_{\perp}(t)$ curves, measured under different conditions of temperature, solvent, excitation wavelength and emission wavelength can be analysed simultaneously (15). An other extension of the global analysis approach was recently suggested by Fendler (16) . In this approach not only the intensity decays $I_{\parallel}(t)$ and $I_{\perp}(t)$ are measured, one makes use of the decays measured under any angle θ of the analyser.

1.3.3. Results

A simulation study was started to find out how one can at best analyse an anisotropy decay. In this simulation study a program was used which allows for different analyser angles to be included in the analysis. This approach was then compared with other methodologies e.g. a global analysis in function of excitation wavelength, emission wavelength or a higher number of counts in the peak channel.

Contradictory to the recent results Fendler (16) presented it was found that the inclusion of more than two analyser angles did not improve the analysis dramatically. An analysis in function of temperature, emission wavelength or excitation wavelength (dependent on the problem) do have a much more pronounced effect on the quality of the analysis.

2. ADSORPTION OF ORGANIC MOLECULES ON SILICA COLLOIDS

2.1 Introduction

The photochemistry and photophysics of adsorbed molecules have gained considerable attention (17). The wide variety of solid surfaces and colloids which have been studied with Py as a probe includes silicas, reversed-phase silica, alumina, titanium, calcium fluoride, semiconductors, clays and zeolites. In the present study, some of the photophysical properties of 3-(1-pyrenyl)propyltrimethylammonium bromide (P3N) adsorbed on a commercially available silica colloid, Ludox^R WP were investigated. The silica particles are modified by replacing some of the surface silicon atoms with aluminum atoms to create a fixed negative charge on the surface independent of pH. Adsorption of P3N on the silica colloid and its mobility on the surface upon addition of co-adsorbed CTAC were studied using photostationary fluorescence and single-photon-timing.

2.2. Excitation and emission spectra

It was already noticed at an early stage (18) that the excimer formation of Py on untreated silica surfaces is more complex than in homogenous solution. It appeared that the excitation spectra measured at the monomer and excimer wavelengths were not identical. This difference ,a red- shift for the spectrum of the excimer with respect to that of the monomer , was taken as a indication that a ground state Py-dimer is present (19).

Fig.1 shows the emission spectrum of P3N adsorbed on Ludox WP. It shows two bands. One with a maximum at 377 nm ascribed to the monomer emission and a second broad band emission with a maximum at 500 nm typical for an excimer emission.

Fig.2 shows the excitation spectra of P3N adsorbed on the colloidal silica Ludox WP (0.1% w/w). It was found that the excitation spectra of excimer-like species is shifted to the red in comparison with the absorption responsible for the monomer-like emission. The influence of co-adsorbed CTAC on the emission of P3N was studied, it was found that upon the addition of co-adsorbent the difference between the excitation spectrum taken in the monomer emission region and that taken in the excimer emission region decreased (fig.3). This indicates a decrease in the groundstate interactions between the chromophors. However, due to the coagulation of the silica at higher CTAC concentrations (from $2 \cdot 10^{-5}$ M on) it is not possible to add a sufficient amount of CTAC to get rid of all the groundstate interactions.

The ratio I_E/I_M of P3N adsorbed on Ludox WP was measured as a function of time. The ratio I_E/I_M decreased from 0.35 to 0.13 for a 0.1 weight percent silica suspension with $6 \cdot 10^{-6}$ M P3N after 40 hours (fig.4).

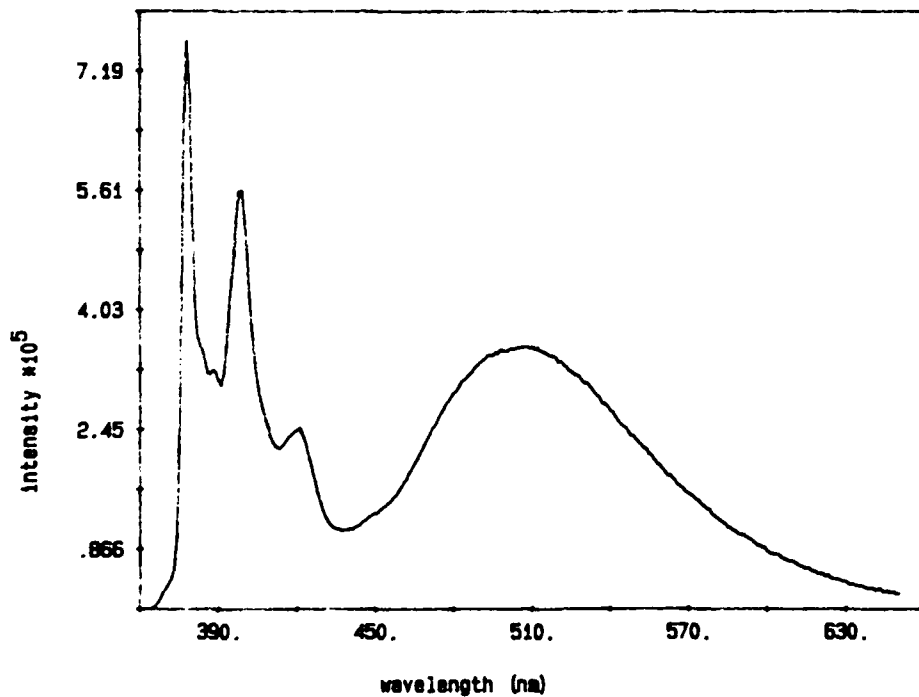


Figure 1 : Emission spectrum of ($6 \cdot 10^{-6}$ M) P3N adsorbed on Ludox Wt 0.1 %

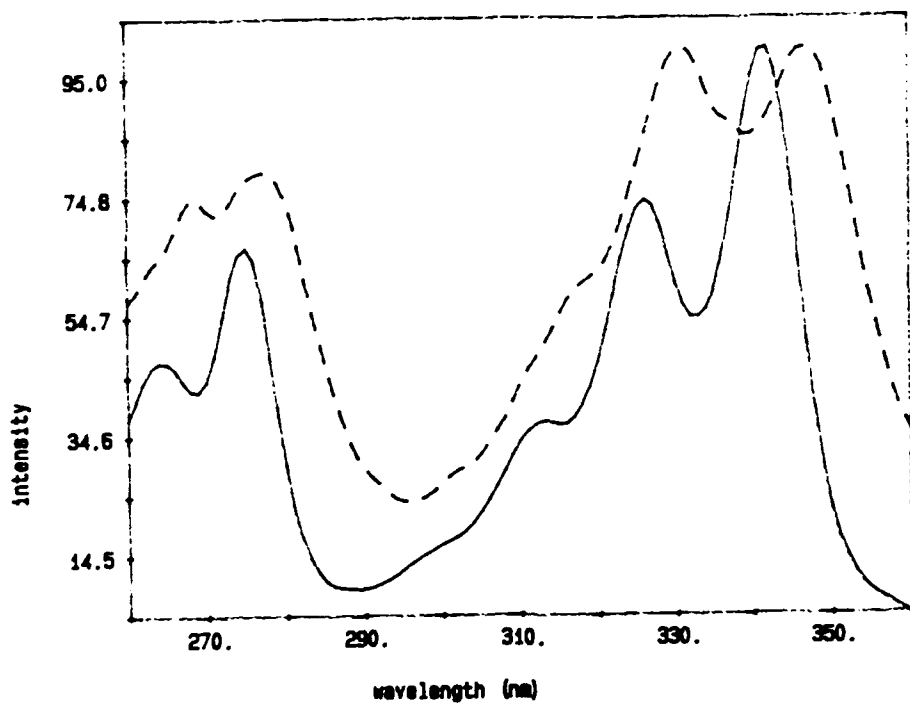


Figure 2 : Excitation spectra of $(6 \times 10^{-6}$ M) P3N adsorbed on Ludox WP 0.1Z
 $(--) I_{em}=378$ nm, (....) $I_{em}=500$ nm.

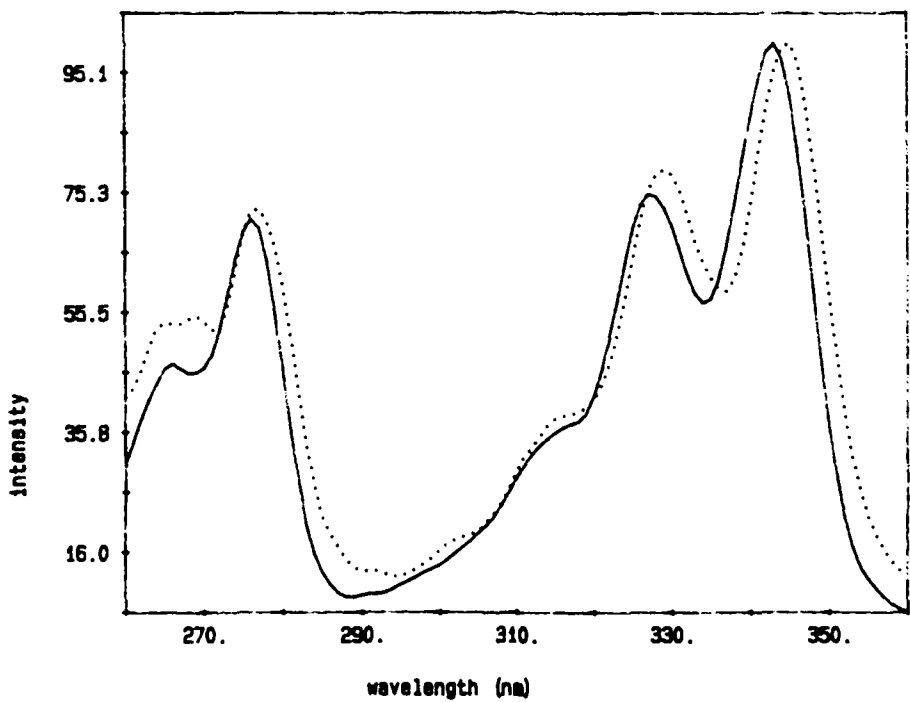


Figure 3 : Excitation spectra of $(6 \times 10^{-6}$ M) P3N adsorbed on Ludox WP 0.1Z
with 5×10^{-5} M CTAC $(--) I_{em}=378$ nm, (....) $I_{em}=500$ nm.

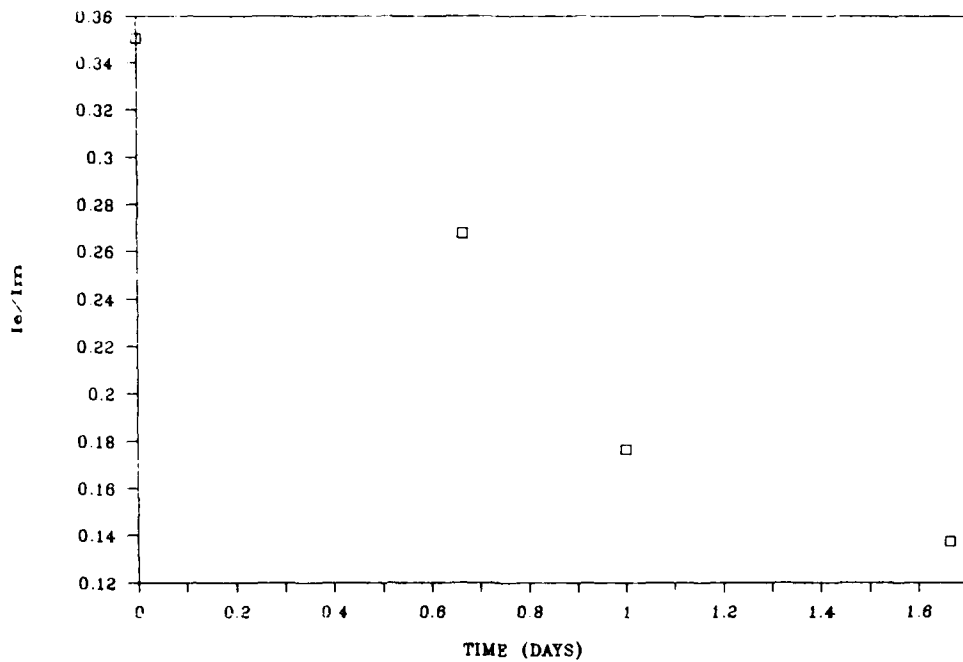


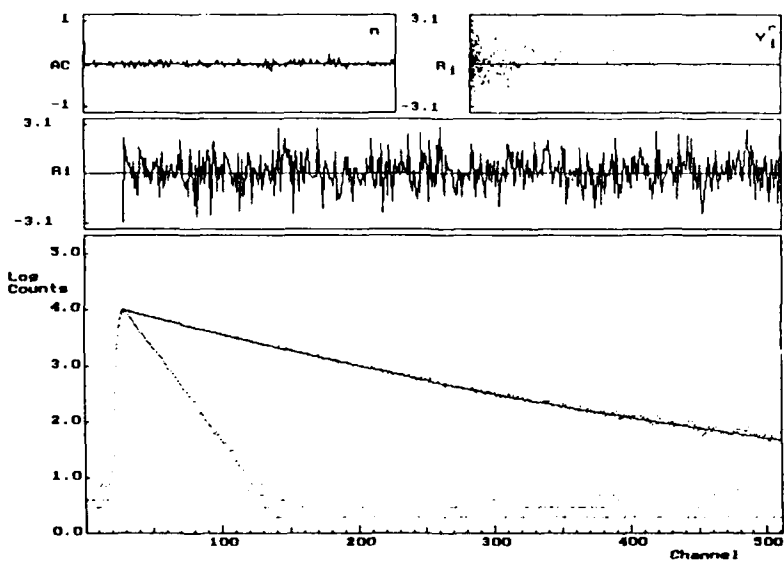
Figure 4 : The ratio I_E/I_M of P3N adsorbed on Ludox WP 0.1% as a function of time

2.3. Decay of adsorbed P3N on silica colloid

The decay of P3N ($6 \times 10^{-6} M$) adsorbed on the silica colloid was nonexponential at the monomer (378 nm) and excimer (487 nm) wavelengths. The analysis was performed assuming a double-exponential decay. Several causes may be examined in an attempt to explain such behaviour: inhomogeneity of the surface, inhomogeneous distribution of the adsorbed chromophores and emission from colloid. The last possibility can be excluded because the measured decay time of silica colloid was found to be very short and of low intensity. The emission from the silica disturbs the fluorescence from adsorbed Py at concentration less than $10^{-8} M/g$ (20). The inhomogeneous interaction between P3N and adsorbing surface seems to be the most reasonable explanation for the multiexponential decay of P3N on silica colloid. The kind of interaction must depend on the nature of the organic molecule adsorbed and on the particular sites of adsorption and the distribution of the negative sites available for adsorption. Different interactions between adsorbate and adsorbent would lead to the formation of different luminescence centers with different deactivation rates of excited state. This with the possibility of

Table 1: Fluorescence decay parameters data of P3N adsorbed on silica colloid WP 0.1%at 378nm.

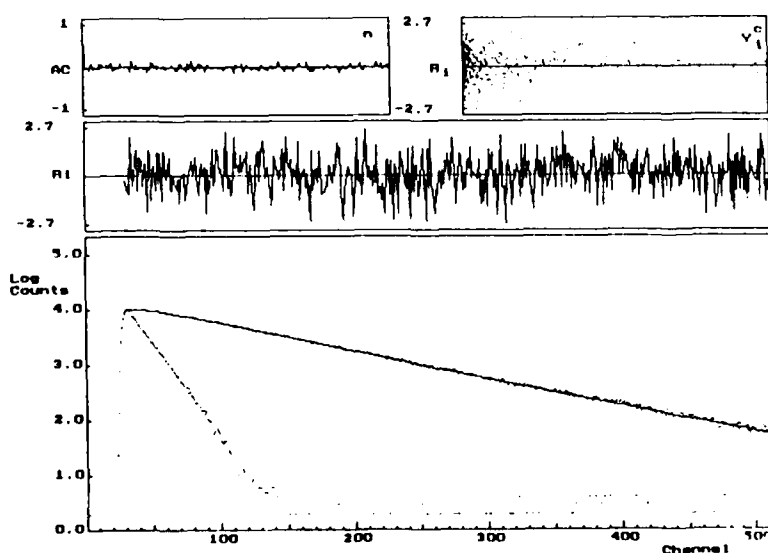
[CTAC] $10^6 M$	A_1	A_2	A_3	A_4	A_5	A_6	χ^2	Z_x^2	$\langle \tau \rangle$
0	0.1866	5.645	0.6754	143.67			1.096	1.071	142.189
12	0.429	9.213	0.442	147.89			1.093	1.443	135.760
At 487nm									
0	0.543	51.51	0.175	9.21	0.0675	105.63	1.06	0.925	60.162
12	-0.068	12.62	0.825	63.929			1.049	0.764	63.094



Reduced chi square = 1.060
 $Z(\chi^2)$ = 0.925
 Ordinary runs test = -0.180
 Durbin-Watson statistic d = 1.997
 Percent of weighted residuals = 93.789
 Mean = 0.029
 S.D. = 1.024

Parameter 1 = 0.54
 Parameter 2 = 51.51
 Parameter 3 = 0.17
 Parameter 4 = 9.21
 Parameter 5 = 0.07
 Parameter 6 = 105.60
 Parameter 7 = 8.25

Figure 5 : Decay curve of the fluorescence of P3N ($6 \cdot 10^{-6}$ M) adsorbed on Ludox WP 0.1 % , exc. = 330nm, em. = 487nm.



Reduced chi square = 1.049
 $Z(\chi^2)$ = 0.764
 Ordinary runs test = -0.106
 Durbin-Watson statistic d = 1.951
 Percent of weighted residuals = 93.568
 Mean = 0.035
 S.D. = 1.021

Parameter 1 = -0.07
 Parameter 2 = 12.63
 Parameter 3 = 0.83
 Parameter 4 = 63.93
 Parameter 5 = 8.25

Figure 6 : Decay curve of the fluorescence of P3N ($6 \cdot 10^{-6}$ M) adsorbed on Ludox WP 0.1 % , with ($1.2 \cdot 10^{-6}$ M) CTAC exc. = 330nm, em. = 487nm.

forming probe cluster on the surface could be responsible for the nonexponential decay. The monomer as well as excimer fluorescence decays of P3N on silica colloid were studied using ($6 \cdot 10^{-6}$ M) of probe and different concentration of CTAC as co-adsorbent to study the effect of co-adsorbent on the photophysical properties of P3N on the surface. Interestingly, the monomer decay is practically double-exponential, and the excimer decay is a triple exponential with a CTAC concentration in the range between zero and $3 \cdot 10^{-6}$ M, and a double exponential in the concentration range $4 \cdot 10^{-6}$ - $1.2 \cdot 10^{-5}$ M (coagulation takes place after that concentration.). A growing-in was found at higher the CTAC concentrations with a amplitude ratio A_{22}/A_{21} not equal to -1 (table 1). This indicates that the addition of CTAC, increases the dynamic excimer formation but most of the excimer still originates from the ground-state dimer. Typical fluorescence decay curves are shown in figs. 5 and 6.

When the CTAC concentration is increased, the hydrophobic environment for the probe increases and part of the excimer is formed dynamically but there is no complete separation of the clusters, as is demonstrated by ratio I_E/I_M which doesn't decrease upon addition of CTAC (fig 7). However, in a treatment of fluorescence decays of molecules adsorbed on solid surfaces such as silica gel (21,22) it was concluded that it is practically impossible, under normal experimental condition, to differentiate a distribution of decay times from two or three separate decay times. It was then argued that it would be difficult to acquire significant information from such decays (23).

2.4 Viscosity measurements

In Fig.8 the viscosity of a silica suspension (0.1%) both with and without adsorbed P3N molecules is given as a function of time. Without probe the viscosity of the silica suspension decreases within the first day after dilution and then stayed constant for over one week. With a probe the viscosity of silica suspension did not change much within the concentrations of silica and probe used.

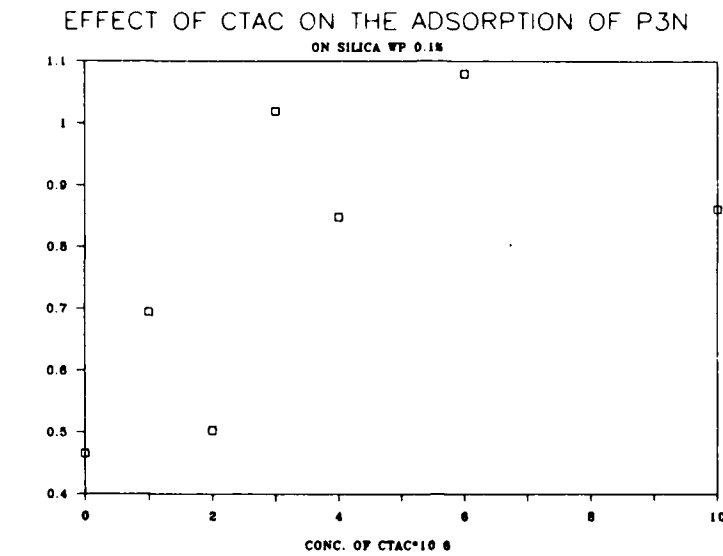


Figure 7 : Effect of co-adsorbed CTAC on the ratio I_E/I_M of P3N on 0.1% WP.

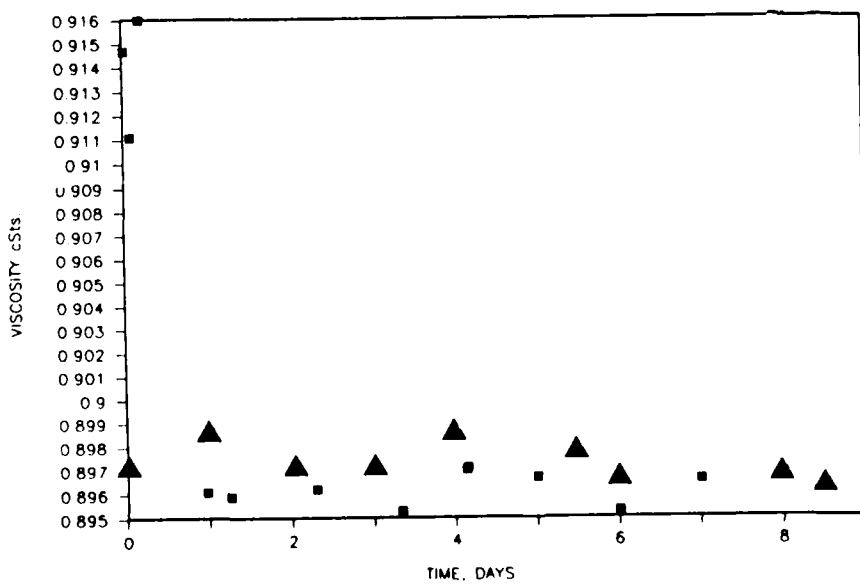


Figure 8 : Viscosity of the silica suspension (0.1%) with (■) and without probe adsorbed to the surface (▲) as a function of time

2.5 Adsorption Isotherm

The determination of the adsorption isotherm of P3N on Ludox WP was carried out as follows : different concentrations of P3N were brought to 10 ml analytical flasks, 5ml of a 0.2% Ludox WP suspension was added and completed to 10 ml with MilliQ water (to get a 0.1 % suspension). the flasks were sonicated for one hour. The suspension was kept under constant temperature for two days to allow for equilibration. These suspensions were then ultracentrifugated for 4 hours. About 6 ml of the supernatant was carefully taken to avoid redispersion. The equilibrium concentration was determined spectrophotometrically at 342nm (fig.9). It was found that at a concentration of 6×10^{-6} M P3N ,which is the concentration used in the experiments, at least 97.5% was adsorbed (0.1% Ludox WP suspension).

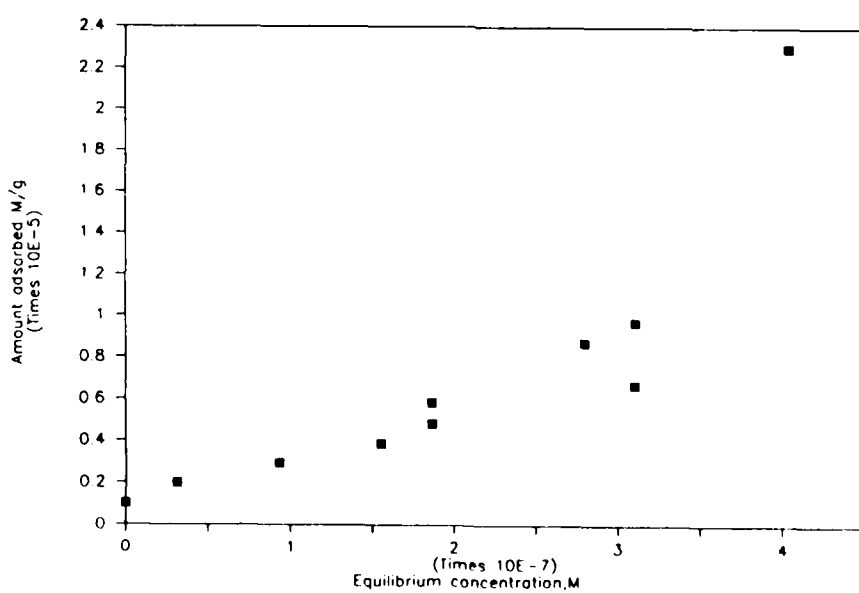


Figure 9 : Adsorption isotherm of P3N on Ludox WP 0.1%

3. SYNTHESIS OF SILICA DERIVATISED WITH A WATER SOLUBLE POLYMER WITH AN UNSATURATED METHACRYLIC BOUND AS END GROUP

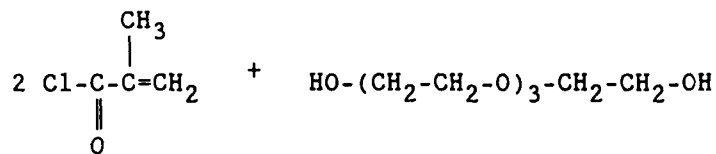
3.1. Introduction

The chemical reaction of an organic moiety with silica can be done as follows:

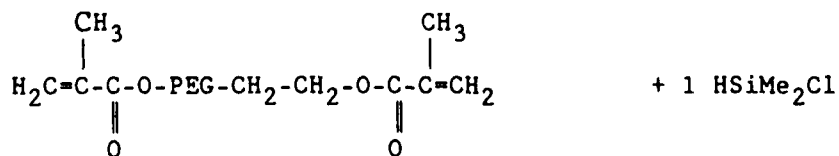
- 1) esterification of the surface silanols, which results in a Si-O-C bound.
- 2) silylation of the surface silanols, which leads to a Si-O-Si-C bound.
- 3) coupling by a Grignard reaction, which results in a Si-C bound.

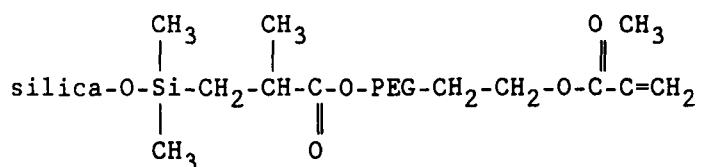
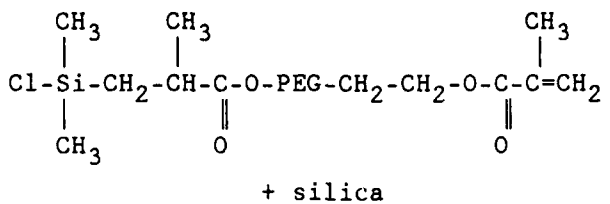
The first reaction leads to a hydrolytic unstable Si-O-C bound, the third reaction is synthetically difficult, thus we have chosen for the silylation of the surface silanols.

3.2. Reactions



methacryloyl-chloride polyethylene glycol (PEG)





3.3 Experimental

3.3.1 Synthesis of polyethylene glycol dimethacrylate (PEGMMA).

0.1 mol of PEG (MG = 200), dried under vacuum at 70 °C is solubilised in 20 ml dichloromethane (CH_2Cl_2). We add 0,4 mol triethylamine and a small amount of 4-hydroxy-2,2,6,6-tetramethyl piperidinoxy free radical (inhibitor) to the solution.

A solution of 0.2 mol methacryloyl chloride is dropwise added to an PEG solution under stirring and cooling. The solution is then stirred at room temperature for 24 hours.

3.3.2. Synthesis of $\text{Cl-Si}(\text{CH}_3)_2-\text{CH}_2-\text{CHCH}_3-\text{CO-O-PEG-O-CO-CCH}_3=\text{CH}_2$.

0.02 mol PEGMMA is solubilised in 20 ml dry toluene. A solution of 0.11 g hydrogen(hexachloroplatinate)hydrate in 2 ml diethylene glycol dimethyl ether and a small amount of 4-hydroxy-2,2,6,6-tetramethyl

piperidinoxy is added. The solution is heated during 1 hour at 60 °C in an oil bath and under argon atmosphere. The oil bath is then removed and a solution of chlorodimethylsilane in toluene is dropwise added to the reaction mixture. The solution is heated for 5 hours at 70 °C under argon atmosphere

3.3.3. Reaction of silica with Cl-Si(CH₃)₂-CH₂-CHCH₃-CO-O-PEG-O-CO-
CCH₃=CH₂.

6 g Silica (Aerosil 300 Degussa), dried for 24 hours under vacuum at 100 °C is dispersed in 250 ml dry toluene, 10 ml pyridine is added. 4g Cl-Si(CH₃)₂-CH₂-CHCH₃-CO-O-PEG-O-CO-CCH₃=CH₂ is added. The mixture is refluxed for 18 hours under argon atmosphere, then stirred for 24 hours at room temperature. The reaction product is filtered. The precipitate is twice dispersed in toluene and filtered. The precipitate is then twice dispersed in dioxane and filtered. The product is dried under vacuum.

3.4. Identification of the reaction product

IR spectroscopy was used to identify the reaction product. the stretching of the carbonyl group can be seen at 1730 cm⁻¹ (figure 10). The presence of the double bound has been verified by reaction with KMnO₄ in neutral environment. Adding of KMnO₄ to an aqueous dispersion of derivatised silica led to a brown colour, while reaction of KMnO₄ with pure Aerosil 300 silica led to a purple colour. A supplementary proof of the unsaturated methacrylic bound has been given by carbon-13 NMR spectroscopy. Figure 11, which represents a carbon -13 spectrum of the derivatised silica in the solid state, resonances at 129 ppm and at 142 ppm are due to the carbons of the double bound.

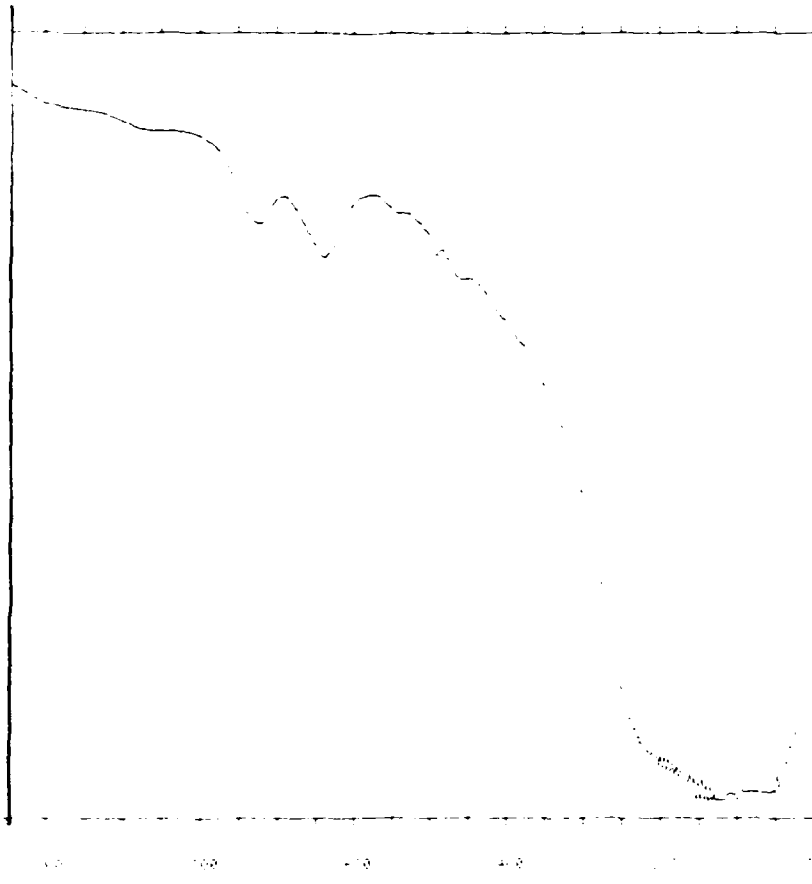


Figure 10 Infrared spectrum of the derivatised silica (KBr disk)

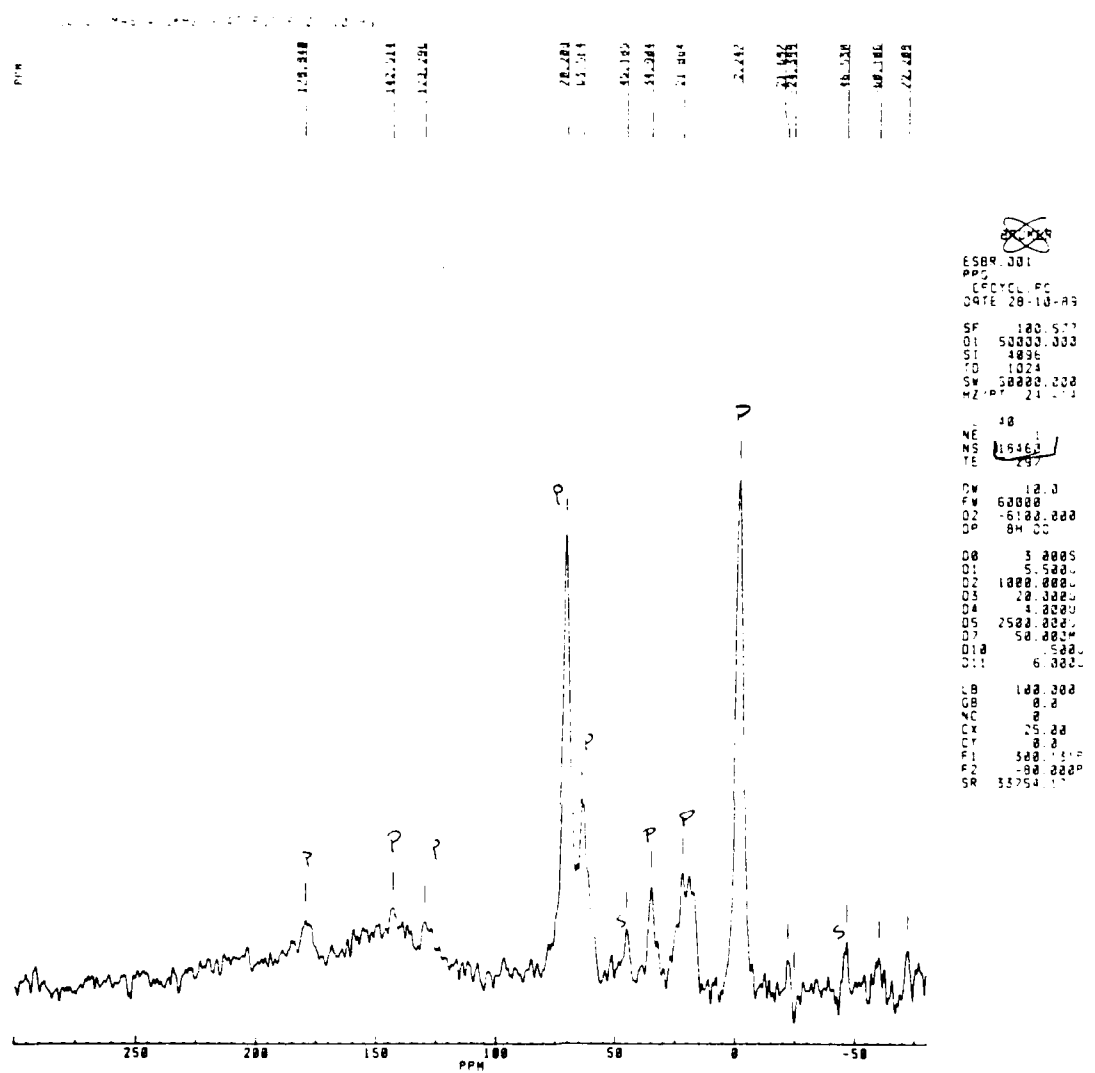


Figure 11 : Solid state ^{13}C -NMR of the derivatised silica

3.5. Polymerisation

Polymerisation by direct irradiation with a high pressure mercury lamp of the product in a quartz tube led to a product which had an IR spectrum where the CO stretching is shifted to higher wavelength. Reaction with KMnO₄ gave a purple colour. Further identification of the resulting polymer is under investigation.

4. ADSORPTION AND POLYMERIZATION OF DETERGENTS AT A CLAY SURFACE

4.1. Absorbance measurements of P3N adsorbed on Laponite : a concentration study

In this study the concentration of the 3-(1-pyrenyl) propyltrimethyl ammonium bromide (P3N) was kept constant. The available surface was changed by varying the concentration of the Laponite. Fig. 12 shows part of the absorption spectra of P3N at the different clay concentrations. The ratio of intensities of the second and the third band of the pyrenyl group of P3N increases as the Laponite concentration increases.(table 2)

Probably this effect is due to a different degree of intermolecular interactions between the chromophors at the different Laponite concentrations.

Table 2 : Ratio of the absorbances of the second and the third band of P3N molecules as a function of Laponite concentration.

[Laponite] g/l	A ₃	A ₂	A ₃ /A ₂	I _e /I _m
0.001	0.026	0.023	1.1304	0.7911
0.005	0.038	0.034	1.1176	1.9268
0.010	0.055	0.050	1.1000	2.5030
0.050	0.066	0.054	1.2222	3.2222
0.080	0.083	0.066	1.2576	3.1887
0.100	0.084	0.063	1.3333	2.3856
0.300	0.090	0.076	1.1842	0.9826
0.500	0.106	0.084	1.2619	1.7165
0.800	0.104	0.075	1.3866	1.6969
1.000	0.111	0.079	1.4051	1.6500

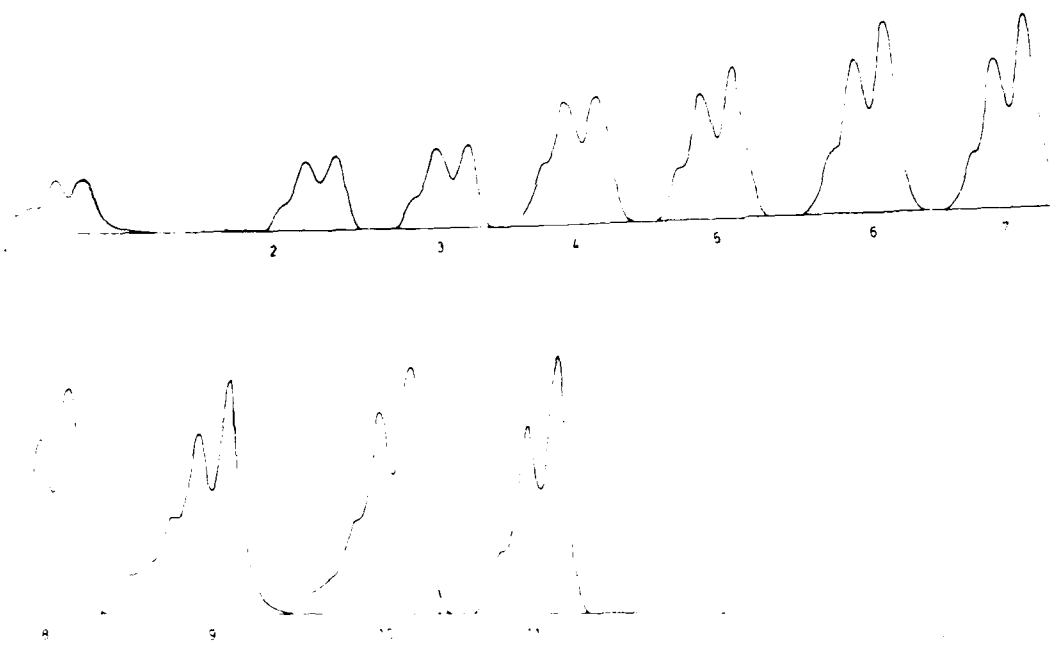


Figure 12 : Pyrene absorption band as a function of clay concentration

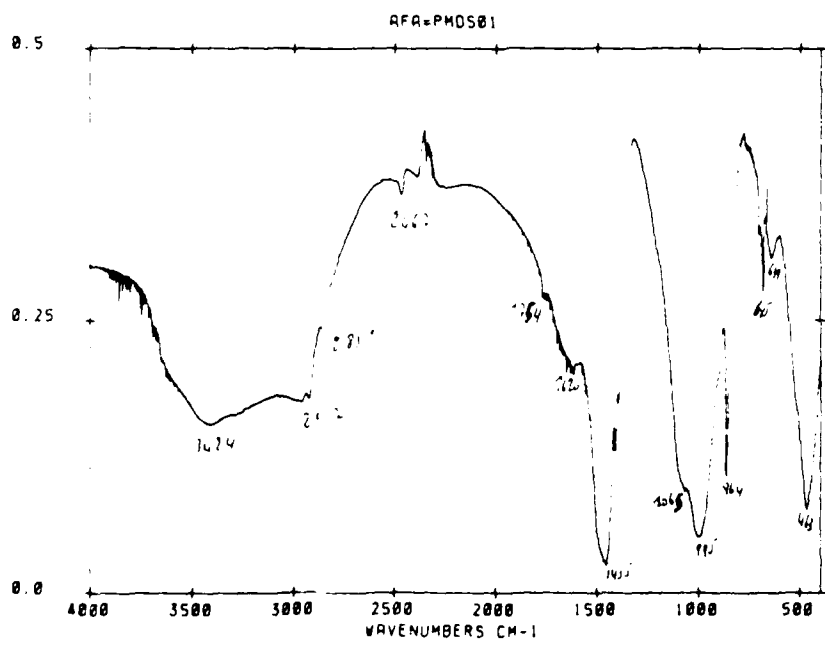


Figure 13 : Infrared spectrum of the Laponite residues (KBr disk)

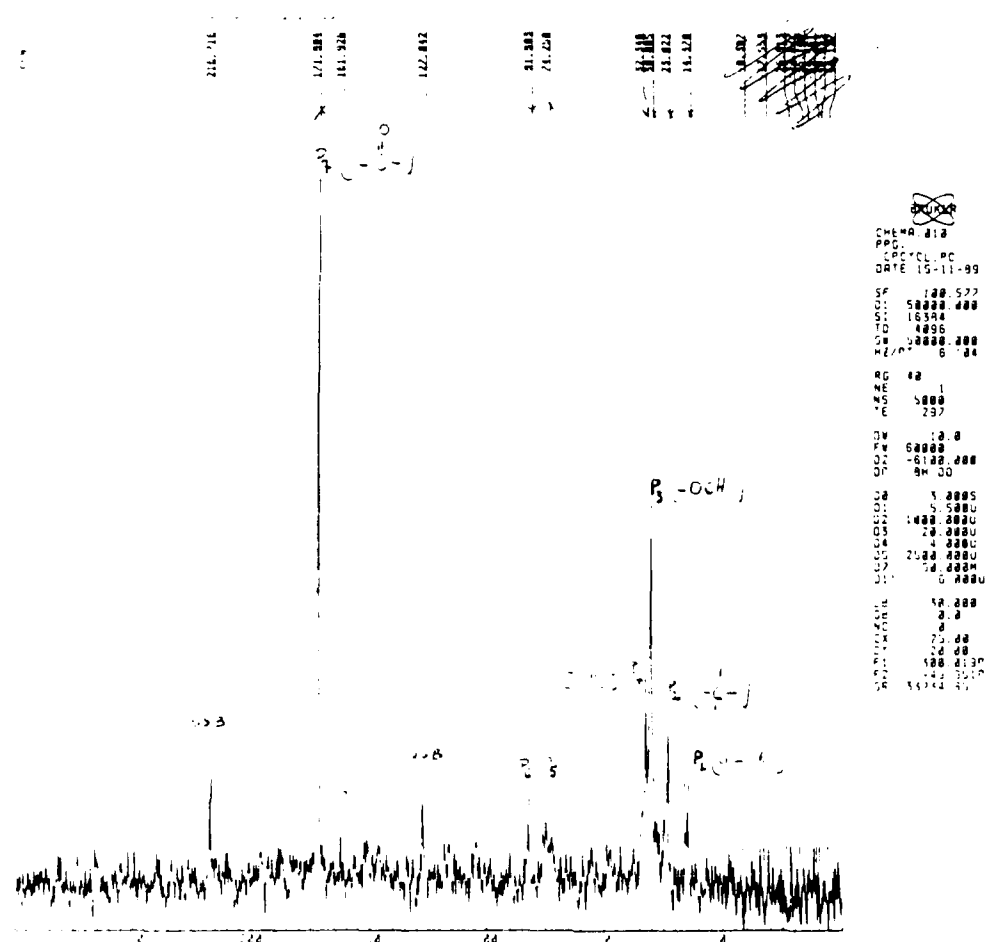


Figure 14 : Solid state ^{13}C -NMR of the Laponite residues

2. Analysis of the residue of the basic hydrolysis.

In our previous report, it has been demonstrated that methacryloyloxyethylmethyldodecylammoniumchloride (DDMEMEC) adsorbed on Laponite surface in water and directly irradiated at 250 nm in quartz cell polymerizes. An attempt has been made to separate polymer from Laponite surface.

A basic hydrolysis has been performed to form polymethacrylic acid. The solution has been centrifuged and the supernatant was analysed. It showed that indeed polymethacrylic acid was present in the solution. Now the Laponite residues were examined.

I.R. and ^{13}C -NMR Spectra (Figures 13 and 14) taken in solid phase, show that there still remains polymer adsorbed on the Laponite surface probably even polymethacrylic acid. Part of the polymer is still strongly attached on the clay surface. It is not yet clear whether this is due to uncomplete hydrolysis or that it is PMMA that remains adsorbed to the clay. Work is in progress to try to vary hydrolysis time in order to detach completely all the polymer on Laponite surface. ^{13}C -NMR spectrum of clay-polymer mixture in solid phase has been compared to ^{13}C -NMR spectrum of polymethacrylic acid taken in DMSO at 25 ° C .

3. Adsorption of polymer from DDMEMEC in toluene on Laponite surface in aqueous suspension

For many systems involving small organic molecules, fairly accurate predictions can be made about the mode of bonding and the orientation of the adsorbed species at the clay surface (24,25). Although the information gained from adsorption studies of short-chain organic species forms the basis for interpreting the behavior of polymeric compounds at clay mineral surfaces, additional variables enter the picture when dealing with organic macromolecules. Besides being long, polymer chains are flexible, multisegmented, and polyfunctional. They

may, therefore, adopt various conformations in solution and become attached to the clay surface by numerous segment-surface bonds.

In addition, accessibility, solubility, and steric factors come into play during the interaction process. Even the order and way in which the components of the system are brought together and mixed can influence the resultant complexes.

As is demonstrated in the previous reports the adsorbed DDMEMEC monomer is polymerisable. If the polymerisation is carried out in the presence of P3N an increase of the excimerband is found. (Figure 15) a comparative study was made to adsorb polymer polymerized in toluene out of the same monomer (DDMEMEC) (with 4,4'- Azobis-(4-cyanovaleric acid as initiator). 0.011 g of the polymer was dissolved in 50 ml of spectroscopic THF to solubilize it. Different amounts of this solution was each time added to a aqueous Laponite suspension. 40 μ l of P3N 10^{-3} M was used as probe.

As with the DDMEMEC monomer a decrease of the ratio Ie/Im of P3N is observed as the polymer concentration increases (Fig. 16); This means that co-adsorption of the polymer results in a decrease of the Ie/Im ratio of the adsorbed P3N. The polymer acts as a diluent and separates the P3N molecules, resulting in a decrease of the relative excimer intensity. This ratio also depends on time (days) (Fig. 17). This can be ascribed to the aggregation of the Laponite particles.

Indeed, the local concentration of polymer will increase upon aggregation, resulting in a better separation of the P3N molecules.

4. Adsorption isotherm of DDMEMEC on Laponite.

An adsorption isotherm for DDMEMEC on Laponite was determined. Different amounts of DDMEMEC were added to a Laponite suspension. The suspensions were left to equilibrate for 24 hours. After centrifugation the (equilibrium) concentration of DDMEMEC in the supernatant was determined by absorbance measurements. The absorbance was measured at 209 nm. A calibration curve was constructed. The

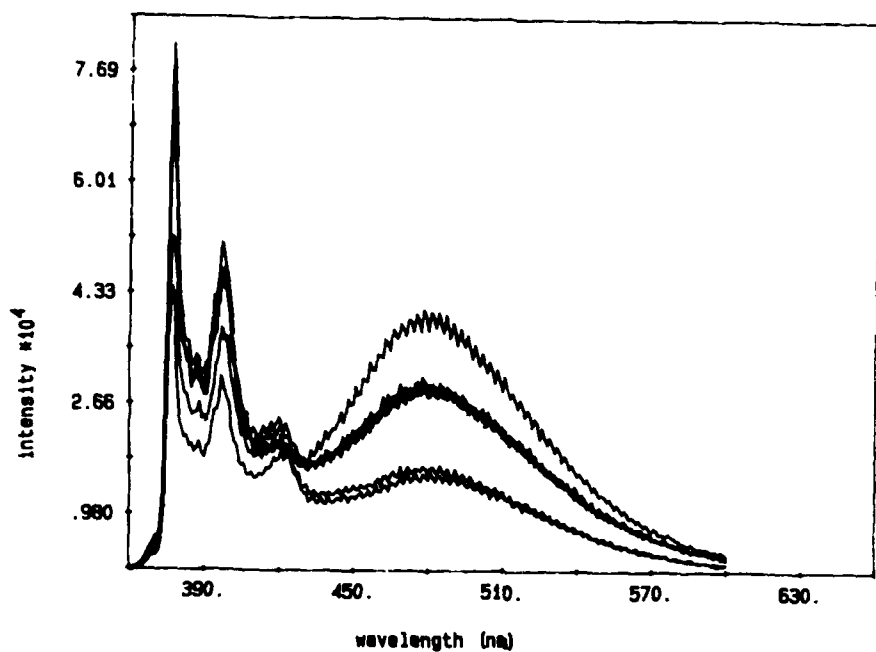


Figure 15 : Emission spectra of P3N on Laponite with DDMEMEC co-adsorbed at different radiation times.

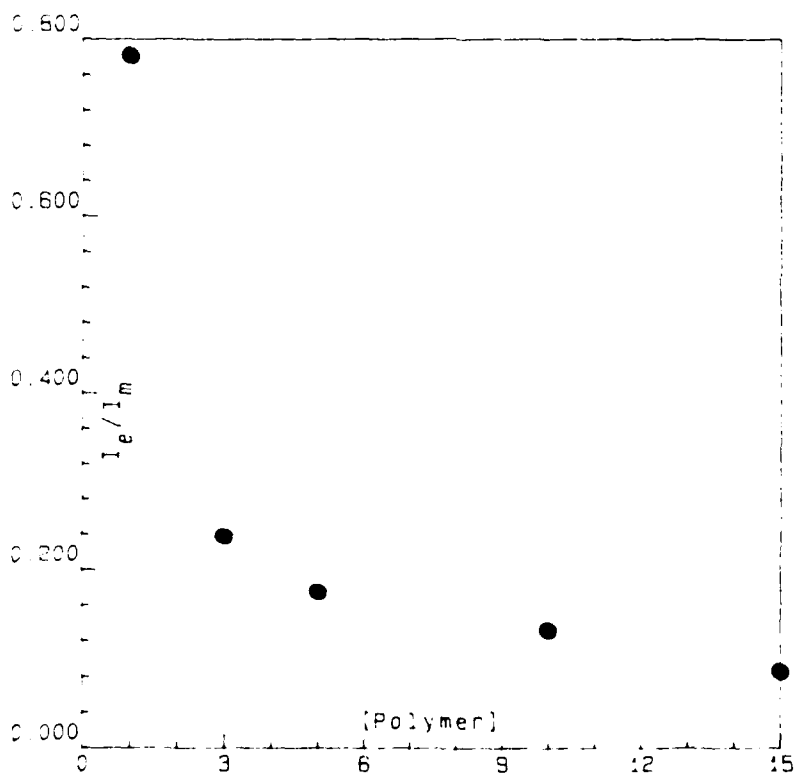


Figure 16 : Variation of the ratio I_E/I_M of P3N as a function of polymer added

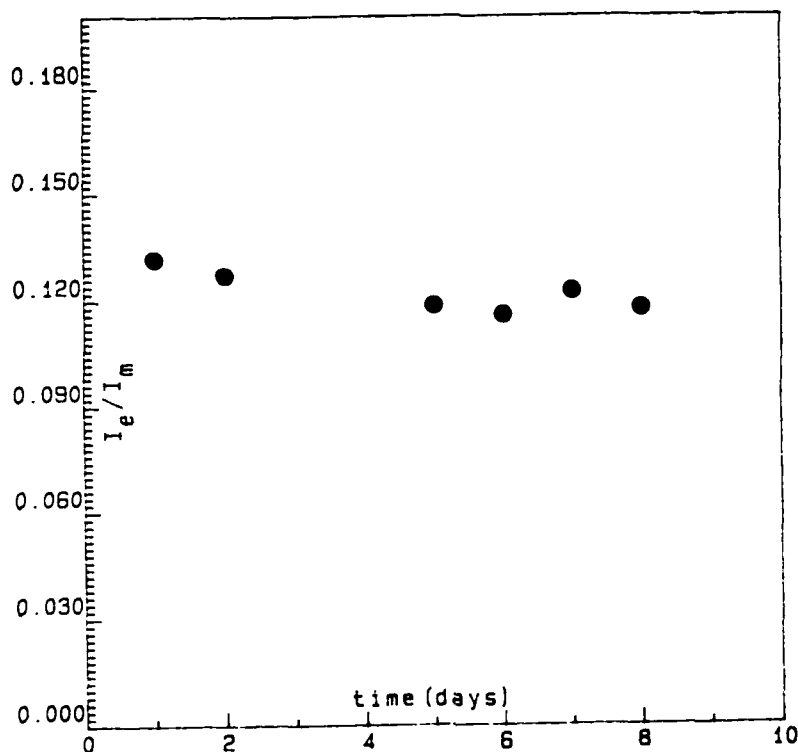


Figure 17 : Variation of the ratio IE/IM of P3N as a function of time
(polymer is added to the solution)

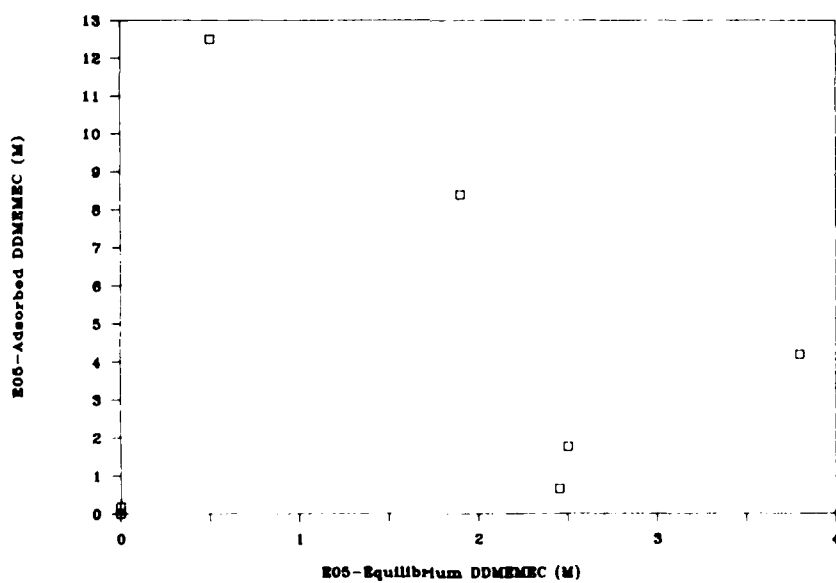


Figure 18 : Adsorption isotherm of DDMEMEC on Laponite

concentration of adsorbed DDMEMEC could be calculated out of the total concentration and the concentration of DDMEMEC in the supernatant.

The obtained isotherm (fig. 18) "turns back" after an initial rise. At higher DDMEMEC concentrations the adsorption is dramatically increased. Thus, from a certain concentration onwards there is another adsorption process working or another species is adsorbed. One possibility is that at that point double layers are formed, the so-called admicelles. In previous reports this admicel formation was already suggested as an explanation for the sudden change in the I_E/I_M ratio at higher loadings and a comparable change in the absorbance at these loadings.

5. REFERENCES

1. Della Guardia, R.A.; Thomas, J.K. *J.Pys. Chem.* 1983, 87, 990.
2. Della Guardia, R.A.; Thomas, J.K. *J.Phys.Chem.* 1984, 88, 964.
3. Nakamura, T.; Thomas, J.K. *J.Phys.Chem.* 1986, 90, 641.
4. Cenens J., PhD thesis KU Leuven, 1988
5. Mandelbrot B., *The fractal geometry of nature*, 1982, Freemann W. and company, San Francisco
6. Klafter J., Blumen A. and Zumofen G., *J. Lum.*, 1984, 31, 627
7. Tamai N.; Yamasaki T. ; Yamasaki I. ; Mizuma A. ; Mataga N., *J. Phys. Chem.*, 1987, 91, 3503
8. Rojanski D. ; Huppert D. ; Avnir D., *Chem. Phys Let.*, 1987, 139, 109
9. Marquardt D.W., *J. Soc. Indust. Appl. Math.*, 1963, 11, 431
10. Tamai N. ; Yamazaki T. ; Yamazaki I., *J. Phys. Chem.*, 1987, 91, 841
11. Perrin F., *J. Phys. Radium*, 1926, 7, 390
12. Jablonski A., *Z. Phys.*, 1935, 96, 390
13. Gilbert C.W., *Time Resolved Fluorescence Spectroscopy in Biochemistry and Biology*, Plenum Press, New York, 1983
14. Cross A. ; Fleming G.R., *Biophys. J.*, 1984, 46, 45
15. Beecham J.M. ; Brand L., *Photochemistry and Photobiology*, 1986, 44, 3, 323
16. Flom S.R. ; Fendhler J.H., *J. Phys. Chem.*, 1988, 92, 5908
17. Avnir D ; Bausse R ; Ottolenghi M ; Weller E ; Zachariasse K.A., *J. Phys. Chem.*, 1985, 89, 3521,.
18. Hara K ; De Mayo P ; Ware W.R. ; Weadon A.C. ; Wong G.S.K. ; Wu K.C., *Chem. Phys. Lett.*, 1988, 89, 105,.
19. Fujii T. ; Shimizu E., *Chem. Phys. Lett.*, 1987, 137, 448,.
20. Bauer R.K. ; De Mayo P ; Ware W.R. ; Wu K.C., *J. Phys.*, 1982, 86, 3781,.
21. James D.R. ; Lin Y-S ; De Mayo P ; Ware W.R., *Chem. Phys. Lett.*, 1985, 120, 460,.
22. James D.R. ; Avnir D., *Langmuir*, 1986, 2, 717,.

23. K.A. Zachariasse in "Photochemistry on solid surfaces"; ed. M. Anpo and T. Masuura, Elsevier, 1989.
24. Theng B.K.G. The chemistry of clay-organic reactions, Adam Hilger Ltd, London, 1974
25. Mortland M.M., *Advan. Agron.*, 1970, 22, 75